Federated Information Mode-Matched Filters in ACC Environment

Yong-Shik Kim and Keum-Shik Hong*

Abstract: In this paper, a target tracking algorithm for tracking maneuvering vehicles is presented. The overall algorithm belongs to the category of an interacting multiple-model (IMM) algorithm used to detect multiple targets using fused information from multiple sensors. First, two kinematic models are derived: a constant velocity model for linear motions, and a constant-speed turn model for curvilinear motions. Fpr the constant-speed turn model, a nonlinear information filter is used in place of the extended Kalman filter. Being equivalent to the Kalman filter (KF) algebraically, the information filter is extended to N-sensor distributed dynamic systems. The model-matched filter used in multi-sensor environments takes the form of a federated nonlinear information filter. In multi-sensor environments, the information-based filter is easier to decentralize, initialize, and fuse than a KF-based filter. In this paper, the structural features and information sharing principle of the federated information filter are discussed. The performance of the suggested algorithm using a Monte Carlo simulation under the two patterns is evaluated.

Keywords: Information filter, interacting multiple model, extended Kalman filter, federated filter, sensor fusion.

1. INTRODUCTION

Recently, the majority of vehicle companies are developing various driver assistance systems to increase vehicle safety and alleviate driver workload. The driver assistance systems include an adaptive cruise control (ACC), a lane-keeping support, a collision warning and collision avoidance, and an assisted lane change. The effectiveness of these driver assistant systems depends on the interpretation of the information arriving from sensors, which provide details of the surrounding vehicle environment and of the driver-assisted vehicle itself. In particular, all these systems rely on the detection and subsequent tracking of objects around the vehicle.

Fig. 1 shows the configuration of an ACC system. The ACC system consists of a driver interface, multisensors which measure the distance and speed of a preceding vehicle, a controller which controls both the throttle and brake, and actuators [13,15]. This ability to predict motions is dependent on how well the sensors of an ACC vehicle can track other vehicles. In order to track other vehicles using the object information obtained from multiple sensors, tracking techniques based on the Bayesian approach are usually used [1]. A number of multiple-model techniques to track a maneuvering target have been proposed in the literature [1,9,10,12,14].

Generally, target motion models can be divided into two subcategories: the uniform motion model and the maneuvering model. A maneuvering target moving at a constant turn-rate and speed is usually modeled as a maneuvering model, and is called a coordinated turn model [1,7-9,14]. For application to air traffic control, a fixed structure IMM algorithm with a single constant velocity model and two coordinated turn models was analyzed [14]. Semerdjiev and Mihaylova [17] discussed variable- and fixed-structure augmented IMM algorithms, whereas a fixed-structure algorithm only was discussed in Li and Bar-Shalom

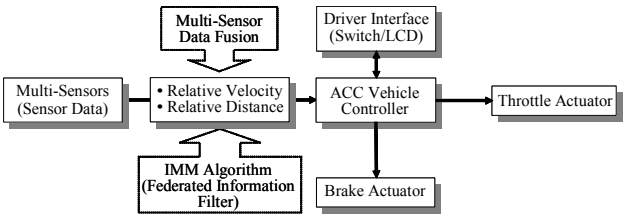

Fig. 1. Configuration of an ACC system.

Manuscript received August 16, 2004; accepted January 12, 2005. Recommended by Editor-in-Chief Myung Jin Chung. This work was supported by the Ministry of Science and Technology of Korea under a program of the National Research Laboratory, grant number NRL M1-0302-00-0039-03-J00-00-023-10 and Research Center for Logistics Information Technology, Pusan National University.

Yong-Shik Kim is with the Graduate School of Systems and Information Engineering, University of Tsukuba, 1-1-1 Tennodai, Tsukuba, Ibaraki 305-8573, Japan (e-mail: kyss@roboken.cs.tsukuba.ac.jp).

Keum-Shik Hong is with the School of Mechanical Engineering, Pusan National University, San 30 Jangjeon-dong Gumjeong-gu, Busan 609-735, Korea (e-mail: kshong@pusan.ac.kr).

* Corresponding author.

[14], and was applied to a maneuvering ship tracking problem by augmenting the turn rate error.

Data fusion techniques are used to employ a number of sensors and to fuse the information from all of these sensors in a central processor [11]. In a distributed system, the processing of raw data is performed at local sensors and the results are transmitted to a data fusion center for track processing in order to obtain the final results. As an alternative method to improve the track fusion, the information filter (IF) [1,16], which is claimed to be the algebraic equivalent to the Kalman filter (KF), was developed. The IF is essentially a KF expressed in measures of information about state estimates and their associated covariances. In addition, a decentralized IF (DIF) was developed by [16]. Carlson [2] and Carlson and Berarducci [3] considered a federated structure as another means of data fusion. It is known that the federated KF (FKF) has the advantages of simplicity and fault-tolerant capability over other decentralized filter techniques.

The contributions of this paper are as follows. First, the IMM algorithm is applied to a driving algorithm for an ACC vehicle in driving on a road in multi-sensor environments. Second, two kinematic models for the possible navigation patterns of vehicle are derived: A constant velocity model for linear motions, and a constant-speed turn model for curvilinear motions. Third, a federated information filter (FIF) for linear motion and a federated nonlinear information filter (FNIF) for curvilinear motion were used in multisensor environments. Fourth, in this study, unlike the FKF, there are no gain or innovation covariance matrices, and the maximum dimension of a matrix to be inverted is the state dimension. Fifth, this paper shows that, in information sharing, the FIF/FNIF is equal to the centralized IF/NIF (CIF/CNIF).

This paper is organized as follows. In Section 2, a stochastic hybrid system is formulated and two kinematic models are discussed. In Section 3, we formulate an FIF for a constant velocity model and an FNIF for a constant-speed turn model in an IMM algorithm in multisensor environments. In Section 4, we evaluate the performance of these filters using a Monte Carlo simulation under the various patterns. Section 5 concludes the paper.

2. PROBLEM FORMULATION

The various driving patterns of a vehicle, such as a straight line and a curve, a cut-in/out, a u-turn, and an interchange were described in [10]. In this section, according to such driving patterns, a stochastic hybrid system in the form of an IMM algorithm to detect other vehicle using multi-sensors is formulated. Also, two kinematic models representing the analyzed driving patterns are introduced.

2.1. Stochastic hybrid system

Following the work of Li and Bar-shalom [14], a stochastic hybrid system with additive noise is considered as follows:

$$\begin{aligned} x(k) &= f[k-1, x(k-1), m(k)] \\ &\quad + g[k-1, x(k-1), \nu[k-1, m(k)], m(k)] \end{aligned} \tag{1}$$

with noisy measurements

$$z(k) = h[k, x(k), m(k)] + w\ [k, m(k)], \tag{2}$$

where $x(k) \in \Re^{n_x}$ is the state vector including the position, velocity, and yaw rate of the vehicle at discrete time k, $m(k)$ is the scalar-valued modal state (driving mode index) at instant k, which is a homogeneous Markov chain with probabilities of transition given by

$$P\{m_j(k+1) \mid m_i(k)\} = \pi_{ij}\ , \qquad \forall m_i, m_j \in \mathrm{M}\ , \tag{3}$$

where $P\{\cdot\}$ denotes the probability and M is the set of modal states, that is, constant velocity, constant acceleration, constant angular rate turning with a constant radius of curvature, among others. The considered system is hybrid since the discrete event $m(k)$ appears in the system. In the driving of ACC vehicle, $m(k)$ denotes the driving mode of the preceding vehicle, in effect during the sampling period ending at k, that is, the time period $(t_{k-1}, t_k]$. The event for which a mode m_j is in effect at time k is denoted as

$$m_j(k) \triangleq \{m(k) = m_j\}\ . \tag{4}$$

$z(k) \in \Re^{n_z}$ is the vector-valued noisy measurement from the sensor at time k, which is mode-dependent. $\nu[k-1, m(k)] \in \Re^{n_\nu}$ is the mode-dependent process noise sequence with mean $\bar{\nu}[k-1, m(k)]$ and covariance $Q[k\text{-}1,\ m(k)]$. $w\ [k, m(k)] \in \Re^{n_z}$ is the mode-dependent measurement noise sequence with mean $\bar{w}[k, m(k)]$ and covariance $R[k, m(k)]$. Finally f, g, and h are nonlinear vector-valued functions.

2.2. Two kinematic models

The concept of using noise-driven kinematic models comes from the fact that noises with different levels of variance can represent different motions. A model with high variance noise can capture maneuvering motions, while a model with low variance noise represents uniform motions. The multiple-models approach assumes that a model can immediately capture the complex system behavior better than others.

Two kinematic models for rectilinear and curvilinear

motions are now derived. First, assuming that accelerations in the steady state are quite small (i.e., abrupt motions like a sudden stop or a collision are not covered), linear accelerations or decelerations can be reasonably well covered by process noises with the constant velocity model. That is, the constant velocity model plus a zero-mean noise with an appropriate covariance representing the magnitude of acceleration can handle uniform motions on the road. In discrete-time, the constant velocity model with noise is given by

$$x(k)=\begin{bmatrix}1 & T & 0 & 0\\ 0 & 1 & 0 & 0\\ 0 & 0 & 1 & T\\ 0 & 0 & 0 & 1\end{bmatrix}x(k-1)+\begin{bmatrix}\frac{1}{2}T^2 & 0\\ T & 0\\ 0 & \frac{1}{2}T^2\\ 0 & T\end{bmatrix}\nu(k-1), \quad (5)$$

where T is the sampling time (i.e., 0.01 sec in this paper), $x(k)$ is the state vector including the position and velocity of the preceding vehicle in the longitudinal (ξ) and lateral (η) directions at discrete time k, that is,

$$x(k)=[\xi(k)\ \dot{\xi}(k)\ \eta(k)\ \dot{\eta}(k)]' \quad (6)$$

with ξ and η denoting the orthogonal coordinates of the horizontal plane; and ν is a zero-mean Gaussian white noise representing the accelerations with an appropriate covariance Q. If $\nu(k)$ is the acceleration increment during the k th sampling period, the velocity during this period is calculated by $\nu(k)T$, and the position is altered by $\nu(k)T^2/2$.

Second, a discrete-time model for turning is derived from a continuous-time model for the coordinated turn motion [1, p. 183]. A constant speed turn is a turn with a constant yaw rate along a road of constant radius of curvature. However, the curvatures of actual roads are not constant. Hence, a fairly small noise is added to a constant-speed turn model for the purpose of capturing the variation of the road curvature. The noise in the model represents the modeling error, such as the presence of angular acceleration and non-constant radius of curvature. For a vehicle turning with a constant angular rate and moving with constant speed (the magnitude of the velocity vector is constant), the kinematic equations in the (ξ,η) plane are

$$\ddot{\xi}(t)=-\omega\dot{\eta}(t), \quad \ddot{\eta}(t)=\omega\dot{\xi}(t) \quad (7)$$

where $\ddot{\xi}(t)$ is the normal (longitudinal) acceleration and $\ddot{\eta}(t)$ denotes the tangential acceleration, and ω is the constant yaw rate (ω > 0 implies a counterclockwise turn). The tangential component of the acceleration is equal to the rate of change of the speed, that is, $\ddot{\eta}(t)=d\dot{\eta}(t)/dt=d(\omega\xi(t))/dt$, and the normal component is defined as the square of the speed in the tangential direction divided by the radius of the curvature of the path, that is, $\ddot{\xi}(t)=-\dot{\eta}^2(t)/\xi(t)=-\omega^2\xi^2(t)/\xi(t)$ where $\dot{\eta}(t)=\omega\xi(t)$. The state space representation of (7) with the state vector defined by $x(t)=[\xi(t)\ \dot{\xi}(t)\ \eta(t)\ \dot{\eta}(t)]'$ becomes

$$\dot{x}(t)=Ax(t), \quad (8)$$

where

$$A=\begin{bmatrix}0 & 1 & 0 & 0\\ 0 & 0 & 0 & -\omega\\ 0 & 0 & 0 & 1\\ 0 & \omega & 0 & 0\end{bmatrix}.$$

The state transient matrix of the system, Eq. (8), is given by

$$e^{At}=\begin{bmatrix}1 & \frac{\sin\omega t}{\omega} & 0 & -\frac{1-\cos\omega t}{\omega}\\ 0 & \cos\omega t & 0 & -\sin\omega t\\ 0 & \frac{1-\cos\omega t}{\omega} & 1 & \frac{\sin\omega t}{\omega}\\ 0 & \sin\omega t & 0 & \cos\omega t\end{bmatrix}. \quad (9)$$

It has been remarked that if the angular rate ω in (7) is time-varying, (9) would be no longer true. In the sequel, following the approach in [1, p. 466], a "nearly" constant-speed turn model in a discrete-time domain is introduced. In this approach, the model itself is motivated from (9), but the angular rate is allowed to vary.

A new state vector by augmenting the angular rate $\omega(k)$ to the state vector of (7) is defined as follows:

$$x^a(k)=[\xi(k)\quad \dot{\xi}(k)\quad \eta(k)\quad \dot{\eta}(k)\quad \omega(k)]' \quad (10)$$

where superscript a denotes the augmented value. Then, the nearly constant-speed turn model is defined as follows [1, p. 467]:

$$x^a(k)=\begin{bmatrix}1 & \frac{\sin\omega(k-1)T}{\omega(k-1)} & 0 & -\frac{1-\cos\omega(k-1)T}{\omega(k-1)} & 0\\ 0 & \cos\omega(k-1)T & 0 & -\sin\omega(k-1)T & 0\\ 0 & \frac{1-\cos\omega(k-1)T}{\omega(k-1)} & 1 & \frac{\sin\omega(k-1)T}{\omega(k-1)} & 0\\ 0 & \sin\omega(k-1)T & 0 & \cos\omega(k-1)T & 0\\ 0 & 0 & 0 & 0 & 1\end{bmatrix}$$
$$\times x^a(k-1)+\begin{bmatrix}T^2/2 & 0 & 0\\ T & 0 & 0\\ 0 & T^2/2 & 0\\ 0 & T & 0\\ 0 & 0 & T\end{bmatrix}\nu^a(k-1). \quad (11)$$

Evidently, both (5) and (11) are special forms of (1).

In addition, it is reasonable to assume that the transition between the driving modes of an ACC vehicle has the Markovian probability governed by (3).

3. FNIF FOR CURVILINEAR MOTIONS

The concept (structure) of an IMM algorithm is referred to in Bar-Shalom *et al*. [1, p.454] and Li and Bar-Shalom [14]. In this study, two models in the IMM algorithm were used: one for rectilinear motions, and the other for curvilinear motions. The tracking procedure of the vehicle in a rectilinear motion, using (5), is carried out by an FIF. However, in tracking curvilinear motions, which requires the estimation of ω with a new augmented model, (8) in Section 2, an FNIF is used.

3.1. The decentralized information filter

We will begin by reviewing the CIF equations [16], as a means of introducing notation, and for later comparison with the FIF equations to be suggested in Section 3.3. Denote the information matrix as $Y(k|k) \overset{\Delta}{=} P^{-1}(k|k)$ and the information state as $\hat{y}(k|k) \overset{\Delta}{=} P^{-1}(k|k)\hat{x}(k|k)$, respectively. Then, at the master filter, assimilation equations to produce the global information state and information matrix with all the sensor data are given as

i) Time update (prediction)

$$\begin{aligned} &\hat{y}(k|k-1) = L(k|k-1)\hat{y}(k-1|k-1), \\ &Y(k|k-1) = [F(k-1)Y^{-1}(k-1|k-1)F'(k-1) \\ &\qquad + Q(k-1)]^{-1}. \end{aligned} \tag{12}$$

ii) Measurement update

$$\begin{aligned} &\hat{y}(k|k) = \hat{y}(k|k-1) + H'(k)R^{-1}(k)z(k), \\ &Y(k|k) = Y(k|k-1) + H'(k)R^{-1}(k)H(k), \end{aligned} \tag{13}$$

where the information prediction coefficient $L(k|k-1)$ is given by

$$L(k|k-1) = Y(k|k-1)F(k-1)Y^{-1}(k-1|k-1). \tag{14}$$

Remark 1: It is preferable to employ an IF since in multi-sensor structures the IF is easier to employ than the KF [16]. The IF is a more direct and natural method of dealing with multi-sensor data fusion problems than the conventional covariance-based KF. The attractive features of the IF are as follows. First, there are no gain or innovation covariance matrices, and the maximum dimension of a matrix to be inverted is the state dimension. In multi-sensor systems, the state dimension is generally smaller than the observation dimension. Hence it is preferable to employ the IF and to invert smaller information matrices than to use the KF and invert larger innovation covariance matrices. Second, initializing the IF is much easier than the KF. This is because information estimates (matrix and state) are easily initialized to zero information. Third, the IF is easier to distribute and fuse than is the KF.

For a local estimate by *j*th sensor, the decentralized estimation equations are given by

i) Time update (prediction)

$$\begin{aligned} &\hat{y}_j(k|k-1) = L_j(k|k-1)\hat{y}_j(k-1|k-1) \\ &Y_j(k|k-1) = [F(k-1)Y_j^{-1}(k-1|k-1)F'(k-1) + Q(k-1)]^{-1}. \end{aligned}, \tag{15}$$

ii) Measurement update

$$\begin{aligned} &\breve{y}_j(k|k) = \hat{y}_j(k|k-1) + H_j'(k)R_j^{-1}(k)z_j(k), \\ &\breve{Y}_j(k|k) = Y_j(k|k-1) + H_j'(k)R_j^{-1}(k)H_j(k), \end{aligned} \tag{16}$$

where the information prediction coefficient $L_j(k|k-1)$ is given by

$$L_j(k|k-1) = Y_j(k|k-1)F(k-1)Y_j^{-1}(k-1|k-1), \tag{17}$$

and $\breve{y}_j(k|k)$ and $\breve{Y}_j(k|k)$ denote the partial information state and its information matrix based only on the *j*th sensor's own observation. Then, the assimilation equations to produce global information estimates are as follows:

i) Information state

$$\hat{y}(k|k) = \hat{y}(k|k-1) + \sum_{j=1}^{N}\{\breve{y}_j(k|k) - \hat{y}_j(k|k-1)\}, \tag{18}$$

ii) Information matrix

$$Y(k|k) = Y(k|k-1) + \sum_{j=1}^{N}\{\breve{Y}_j(k|k) - Y_j(k|k-1)\}. \tag{19}$$

Remark 2: As an alternative filtering method of the CIF, the DIF was suggested [5]. In this study, however, contrary to the fully connected decentralized estimation algorithm of Mutambara [16], there was no communication between sensors in the filter structure. In Chong *et al*. [6] and Zhu *et al*. [18], Kalman-filtering fusion with feedback from a central processor in a decentralized architecture is shown. It is composed of multiple structures involving a master filter at high level and local filters at low level. A local filter, related to each observation sensor, estimates the local state variable. The master filter combines the estimates transmitted from the local filters and deduces the globally optimal state estimate. A decentralized filter presented in this paper employs the architecture proposed in Chong *et al*. [6] and Zhu *et al*. [18]. As explained earlier, the decentralized estimation algorithm has the same form as the

centralized estimation algorithm in real-time implementation, since the master model includes N estimates. In general, however, in the event that the system models at local filters are all the same and the observation model is decomposed to each local filter, the filter structure is not optimal. The estimate of a local filter is affected by the overlapping use of the system model. The end result is that the computational load can be significantly reduced by this decentralized technique. Although the decentralized filtering technique has been recognized as an effective method of reducing the typically high computational load in standard centralized filtering, its potentially high fault-tolerance performance capability has not been widely investigated.

3.2. The FIF for the constant velocity model

An FKF can be considered a special form of decentralized KF [3]. The federated filter takes the decentralized technique one step further by employing the information-sharing principle. The federated filter can obtain the globally optimal estimate by applying the information-sharing principle to each local filter and then fusing the estimates of these local filters. For the systems of a local filter structure such as (15) and (16), the global information matrix and information state equations are as follows:

$$Y_{master}(k \mid k) = Y_1(k \mid k) + \cdots + Y_N(k \mid k), \tag{20}$$

$$\hat{y}_{master}(k \mid k) = \sum_{i=1}^{N} \hat{y}_i(k \mid k). \tag{21}$$

Theorem 1: For the system (1) and (2), and the local filter structure (15) and (16), the solution of the FIF, (20) and (21), is equal to the solution of the CIF, (12) and (13), if conditions a) - c) are satisfied.

a) The initial value of the information matrix, the initial information state, and the process noise covariance are distributed to local filters as follows:

$$Y_i(0 \mid 0) = \frac{1}{\gamma_i} Y(0 \mid 0), \quad i = 1, \cdots, N, \tag{22}$$

$$\hat{y}_i(0 \mid 0) = Y^{-1}(0 \mid 0) Y_i^{-1}(0 \mid 0) \hat{y}(0 \mid 0), \quad i = 1, \cdots, N, \tag{23}$$

$$Q_i(k) = \gamma_i Q(k), \quad i = 1, \cdots, N. \tag{24}$$

b) The information state and its information matrix, which are calculated using (20) and (21), are distributed to the local filters as follows:

$$Y_i(k \mid k) = \frac{1}{\gamma_i} Y_{master}(k \mid k), \quad i = 1, \cdots, N, \tag{25}$$

$$\hat{y}_i(k \mid k) = \hat{y}_{master}(k \mid k), \quad i = 1, \cdots, N. \tag{26}$$

c) An information-sharing factor is defined as follows:

$$\sum_{i=1}^{N} \frac{1}{\gamma_i} = 1, \quad 0 \le \frac{1}{\gamma_i} \le 1. \tag{27}$$

Proof: we shall prove this hypothesis using a mathematical induction. First, we assume that at the k-1 time epoch, the information state and the information matrix of the master filter is identical to those of the CIF as follows:

$$Y_{master}(k-1 \mid k-1) = Y^*(k-1 \mid k-1), \; i=1, \cdots, N, \tag{28}$$

$$\hat{y}_{master}(k-1 \mid k-1) = \hat{y}^*(k-1 \mid k-1), \; i=1, \cdots, N, \tag{29}$$

where $\hat{y}^*$ and Y^* are the information state and its information matrix of the CIF, respectively. The fused information state and its information matrix are sent to the local filters as follows:

$$Y_i(k-1 \mid k-1) = \frac{1}{\gamma_i} Y_{master}, \tag{30}$$

$$\hat{y}_i(k-1 \mid k-1) = \hat{y}_{master}(k-1 \mid k-1). \tag{31}$$

The prediction procedure at each local filter, using (12) and (13) of the CIF, is rewritten as follows:

$$\begin{aligned} Y_i(k \mid k-1) &= [F(k-1)\{Y_i(k-1 \mid k-1)\}^{-1} \\ &\quad F'(k-1) + Q_i(k-1)]^{-1} \\ &= [F(k-1)\{\frac{1}{\gamma_i} Y_{master}(k-1 \mid k-1)\}^{-1} F'(k-1) + \gamma_i Q(k-1)]^{-1} \\ &= \frac{1}{\gamma_i} [F(k-1) Y_{master}^{-1}(k-1 \mid k-1) F'(k-1) + Q(k-1)]^{-1} \\ &= \frac{1}{\gamma_i} [F(k-1) Y^{-1*}(k-1 \mid k-1) F'(k-1) + Q(k-1)]^{-1} \\ &= \frac{1}{\gamma_i} Y^*(k \mid k-1), \qquad i = 1, \cdots, N, \end{aligned} \tag{32}$$

$$\begin{aligned} \hat{y}_i(k \mid k-1) &= L_i(k \mid k-1) \hat{y}_i(k-1 \mid k-1) \\ &= L_i(k \mid k-1) \hat{y}_{master}(k-1 \mid k-1) \\ &= L_i(k \mid k-1) \hat{y}^*(k-1 \mid k-1) \\ &= \hat{y}^*(k \mid k-1). \end{aligned} \tag{33}$$

The measurement update of the information matrix at each local filter can be obtained as follows:

$$\begin{aligned} Y_i(k \mid k) &= Y_i(k \mid k-1) + H_i'(k) R_i^{-1}(k) H_i(k) \\ &= \frac{1}{\gamma_i} Y_{master}(k \mid k-1) + H_i'(k) R_i^{-1}(k) H_i(k). \end{aligned} \tag{34}$$

Hence, the assimilation equation in the master filter is expressed as follows:

$$\begin{aligned} Y_{master}(k \mid k) &= \sum_{i=1}^{N} Y_i(k \mid k) \\ &= \sum_{i=1}^{N} \frac{1}{\gamma_i} Y_{master}(k \mid k-1) + \sum_{i=1}^{N} H_i'(k) R_i^{-1}(k) H_i(k) \end{aligned}$$

$$= Y(k \mid k-1) + \sum_{i=1}^{N} H_i'(k) R_i^{-1}(k) H_i(k) \quad (35)$$
$$= Y(k \mid k).$$

The measurement update of the information state at the local filters can be written as

$$\hat{y}_i(k \mid k) = \hat{y}_i(k \mid k-1) + H_i'(k) R_i^{-1}(k) z_i(k). \quad (36)$$

Therefore, the assimilation equation in the master filter is given by

$$\begin{aligned} \hat{y}_{master} &= \hat{y}_1 + \cdots + \hat{y}_N = \sum_{i=1}^{N} \hat{y}_i(k \mid k) \\ &= \sum_{i=1}^{N} [\hat{y}_i(k \mid k-1) + H_i'(k) R_i^{-1}(k) z_i(k)] \\ &= \hat{y}^*(k \mid k-1) + \sum_{i=1}^{N} H_i'(k) R_i^{-1}(k) z_i(k) \\ &= \hat{y}^*(k \mid k). \end{aligned} \quad (37)$$

Remark 3: According to (22) and (24) of the suggested filtering scheme, the system process information is distributed among the master and local filters in the proportion of $1/\gamma_i$. The issue in the suggested filter design is to determine how the total information is to be divided among the individual filters to achieve a higher fault-tolerance performance and improvement in throughput and efficiency. In the suggested filter, contrary to the other decentralized filters, the master filter combines only the filtered information state and its information matrix of local filters. Therefore, the number of variables transmitted from the local filters to the master filter is diminished. The FIF structure is shown in Fig. 2.

3.3. The FNIF for the constant-speed turn model

Since the model in (11) is nonlinear, the estimation of the state equation (10) will be performed via the FNIF. The nearly constant-speed turn model of (11) can be rewritten as follows:

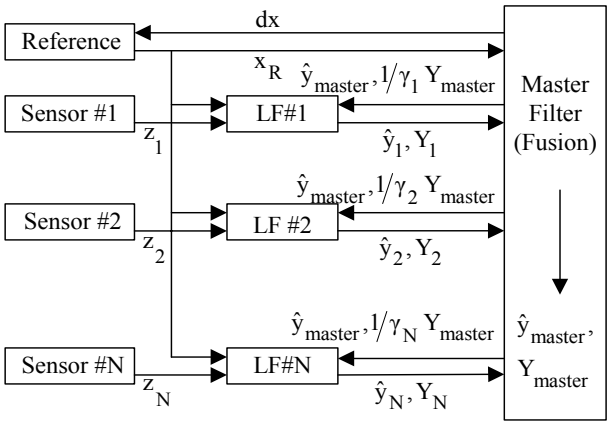

Fig. 2. FIF structure.

$$x^a(k) = f^a[x^a(k-1), \omega(k-1)] + G(k-1)v^a(k-1), \quad (38)$$

where the function $f^a(\cdot)$ is known and remains unchanged during the estimation procedure. The noise transition matrix $G(k-1)$ is the same form as that given in (11). To obtain the predicted state $\hat{x}^a(k \mid k-1)$, the nonlinear function in (38) is expanded in Taylor series around the latest estimate $\hat{x}^a(k-1 \mid k-1)$ with terms up to first order, to yield the first-order EKF. The vector Taylor series expansion of (38) up to first order is

$$\begin{aligned} x^a(k) = f^a[\hat{x}^a(k-1 \mid k-1), \omega(k-1)] + f^a_{x^a}(k-1) \\ \times [x^a(k-1) - \hat{x}^a(k-1 \mid k-1)] \\ + \mathrm{HOT} + G(k-1)v^a(k-1), \end{aligned} \quad (39)$$

where HOT represents the higher-order terms and

$$f^a_{x^a}(k-1) = [\nabla_{x^a} f^a(x^a, \omega)']' \mid_{x^a = \hat{x}^a(k-1 \mid k-1)}$$
$$= \begin{bmatrix} 1 & \frac{\sin \hat{\omega}(k-1)T}{\hat{\omega}(k-1)} & 0 & -\frac{1-\cos \hat{\omega}(k-1)T}{\hat{\omega}(k-1)} & f_{\omega,1}(k-1) \\ 0 & \cos \hat{\omega}(k-1)T & 0 & -\sin \hat{\omega}(k-1)T & f_{\omega,2}(k-1) \\ 0 & \frac{1-\cos \hat{\omega}(k-1)T}{\hat{\omega}(k-1)} & 1 & \frac{\sin \hat{\omega}(k-1)T}{\hat{\omega}(k-1)} & f_{\omega,3}(k-1) \\ 0 & \sin \hat{\omega}(k-1)T & 0 & \cos \hat{\omega}(k-1)T & f_{\omega,4}(k-1) \\ 0 & 0 & 0 & 0 & 1 \end{bmatrix} \quad (40)$$

is the Jacobian of the vector f evaluated with the latest estimate of the state. The partial derivatives with respect to ω are given by

$$\begin{aligned} f_{\omega,1} &= \frac{T\hat{\dot{\xi}}(k-1 \mid k-1)\cos \hat{\omega}(k-1)T}{\hat{\omega}(k-1)} \\ &\quad - \frac{\hat{\dot{\xi}}(k-1 \mid k-1)\sin \hat{\omega}(k-1)T}{\hat{\omega}(k-1)^2} \\ &\quad - \frac{T\hat{\dot{\eta}}(k-1 \mid k-1)\sin \hat{\omega}(k-1)T}{\hat{\omega}(k-1)} \\ &\quad - \frac{\hat{\dot{\eta}}(k-1 \mid k-1)(-1+\cos \hat{\omega}(k-1)T)}{\hat{\omega}(k-1)^2}, \\ f_{\omega,2} &= -T\hat{\dot{\xi}}(k-1 \mid k-1)\sin \hat{\omega}(k-1) \\ &\quad - T\hat{\dot{\eta}}(k-1 \mid k-1)\cos \hat{\omega}(k-1), \\ f_{\omega,3} &= \frac{T\hat{\dot{\xi}}(k-1 \mid k-1)\sin \hat{\omega}(k-1)T}{\hat{\omega}(k-1)} \\ &\quad - \frac{\hat{\dot{\xi}}(k-1 \mid k-1)(1-\cos \hat{\omega}(k-1)T)}{\hat{\omega}(k-1)^2} \\ &\quad + \frac{T\hat{\dot{\eta}}(k-1 \mid k-1)\cos \hat{\omega}(k-1)T}{\hat{\omega}(k-1)} \end{aligned} \quad (41)$$

$$-\frac{\hat{\dot{\eta}}(k-1|k-1)\sin\hat{\omega}(k-1)T}{\hat{\omega}(k-1)^2},$$

$$f_{\omega,4} = T\hat{\dot{\xi}}(k-1|k-1)\cos\hat{\omega}(k-1) - T\hat{\dot{\eta}}(k-1|k-1)\sin\hat{\omega}(k-1),$$

where Q^a is the covariance of the process noise in (38).

For a local estimate by the j th sensor, the decentralized nonlinear estimation equations are given by

i) Time update (prediction)

$$\hat{y}_j(k|k-1) = Y_j(k|k-1) f^a[\hat{x}_j^a(k-1|k-1), \omega(k-1)],$$
$$Y_j(k|k-1) = [f_{x^a}^a(k-1) Y_j^{-1}(k-1|k-1) f_{x^a}'^a(k-1) + Q^a(k-1)]^{-1}. \quad (42)$$

ii) Measurement update

$$\breve{y}_j(k|k) = \hat{y}_j(k|k-1) + h_{x^a}'^a(k) R_j^{-1}(k)[\upsilon_j(k) + h_{x^a}^a(k)\hat{x}_j^a(k|k-1)], \quad (43)$$
$$\breve{Y}_j(k|k) = Y_j(k|k-1) + h_{x^a}'^a(k) R_j^{-1}(k) h_{x^a}^a(k),$$

where $h_{x^a}^a(k) = [\nabla_{x^a} h^a(x^a, \omega)']'|_{x^a=\hat{x}^a(k|k-1)}$ is the Jacobian of the vector h^a evaluated at the predicted state $\hat{x}^a(k|k-1)$, and $\upsilon(k)$ is the innovation given by $\upsilon(k) = z(k) - h^a(k, \hat{x}^a(k|k-1), w(k))$. Then, the assimilation equations to produce global information estimates are as follows:

i) Information state

$$\hat{y}_{master}(k|k) = \sum_{i=1}^{N} \breve{y}_i(k|k), \quad (44)$$

ii) Information matrix

$$Y_{master}(k|k) = \breve{Y}_1(k|k) + \cdots + \breve{Y}_N(k|k). \quad (45)$$

Remark 4: Ultimately, the local filters in the FNIF produce the same results as the information state and information matrix of the DIF, (15) and (16). However, the assimilation equations of the master filter produce the global optimal value by using only the updated value of each local filter.

4. SIMULATIONS RESULTS

As described in this section, we considered a state estimation problem of a vehicle in two dimensions. Simulations were executed to compare the performance of the IMM algorithms using a centralized EKF (CEKF), a federated EKF (FEKF), a centralized nonlinear IF (CNIF), and an FNIF, respectively, for curvilinear motions. The performance of these four algorithms was compared with the use of Monte Carlo simulations. The maneuvering vehicle trajectories were generated using the various patterns mentioned in [10]. Two kinematic models were used to track the maneuvering vehicle: A constant-velocity model for rectilinear motions and a constant-speed turn model for curvilinear motions. We then compared the performance of the four different IMM algorithms with these two models.

4.1. The driving scenarios

It was assumed that the vehicle moves rectilinearly in the beginning. The target initial positions and velocities were differently set for each scenario. The single-target track of the maneuvering vehicle was also assumed to have been previously initialized and that track maintenance was the goal of the IMM algorithms. The results for the 4 selected scenarios are presented, according to the driving patterns.

i) Scenario for straight line and curve: The target initial positions and velocities were (x_0= 0 m; y_0=0 m; $\dot{x}_0$ =28 m/s; $\dot{y}_0$ =28 m/s; ω =0°/s). Its trajectory was a constant velocity between 0 s and 180 s with a speed of 28 m/s; a turn with a constant yaw rate of ω = 1.4°/s between 180 s and 225 s; a constant velocity between 225 s and 362 s; a turn with a constant yaw rate of ω = 1.4°/s between 362 s and 437 s; a constant velocity between 437 s and 615 s.

ii) Cut-in/out scenario: The target initial positions and velocities were (x_0=0 m; y_0=20 m; $\dot{x}_0$ = 28 m/s; $\dot{y}_0$ =0 m/s; ω=0°/s). Its trajectory was a straight line between 0 s and 73 s with a speed of 28 m/s; a turn with a constant yaw rate of ω = 5.6°/s between 73 s and 82 s; a constant velocity between 82 s and 104 s with a speed of 28 m/s; a turn between 104 s and 113 s with a yaw rate of ω = 5.6°/s; a straight line between 113 s and 149 s with a speed of 28 m/s; a turn with a constant yaw rate of ω = 5.6°/s between 149 s and 158 s; a constant velocity between 158 s and 180 s with a speed of 28 m/s; a turn between 180 s and 189 s with a yaw rate of ω = 5.6°/s, and a straight line between 189 s and 260 s.

iii) U-turn scenario: The target initial positions and velocities were (x_0=10 m; y_0=10 m; $\dot{x}_0$ =28 m/s; $\dot{y}_0$ =0 m/s; ω =0°/s). This scenario included a non-maneuvering driving mode during scans from 0 s to 73 s with a speed of 28 m/s, a 180° turn, lasting from scan 73 s to 107 s with a yaw rate of ω=9.3°/s, and a non-maneuvering driving mode from scan 107 s to 178 s.

iv) Interchange scenario: The target initial positions and velocities were (x_0=0 m, y_0=0 m, $\dot{x}_0$ =28 m/s, $\dot{y}_0$ =0 m/s, ω =0°/s). This scenario included a non-maneuvering driving mode during scans from 0 s to 144 s with a speed of 28 m/s, a 270°-turn, lasting from scan 144 s to 481 s with a yaw rate of ω =1. 4°/s, and

a non-maneuvering driving mode from scan 481 s to 624 s. The maneuvering vehicle speed was 28 m/s.

4.2. Parameters used in the design

The parameters used in the design are listed here. Subscripts "CV" and "CST" stand for "constant velocity" and "constant speed turn," respectively. The initial yaw rate of each navigation scenario was $\omega(0)$=-1.4°/s, -5.6°/s, 9.3°/s, and –1.4°/s, respectively. The initial values of information matrix were as follows:

CV mode: $Y(0|0) = \text{diag}\{1 \quad 0.5 \quad 1 \quad 0.5\}$,

CST mode: $Y(0|0) = \text{diag}\{1 \quad 0.5 \quad 1 \quad 0.5 \quad \sigma_\omega^2\}$,

where σ_ω = (0.1) °/s. The information sharing factors used for the two sensors were $1/\gamma_1 = 1/\gamma_2 = 0.5$. The initial mode probability vectors μ were chosen as follows:

$$\mu = \begin{bmatrix} 0.5 \\ 0.5 \end{bmatrix}.$$

4.3. Performance evaluation and analysis

The RMS error of each state component was chosen as the measure of performance. The comparison results of the IMM algorithms using a CEKF, an FEKF, a CNIF, and an FNIF, respectively, for the curvilinear motion are shown in Figs. 3-14, where the RMS error in the position and the velocity are plotted by Figs. 4, 5, 7, 8, 10, 11, 13, and 14. Figs. 3, 6, 9, and 12 show comparisons of the true position and the estimated ones with the CEKF, the FEKF, the CNIF, and the FNIF, respectively. The results presented here are based on 100 Monte Carlo runs. It is evident that the two algorithms have almost equal position and velocity estimation accuracy for all scenarios. This confirms the algebraic equivalence which is mathematically proven and established in the derivation of the information filter from the Kalman filter. These conclusions were confirmed by the RMS error plots presented in Figs. 3-14, respectively.

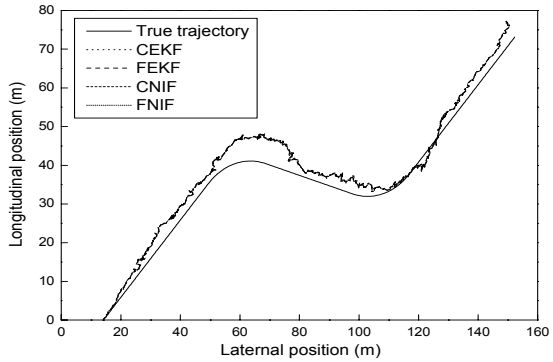

Fig. 3. Comparison of position estimates in the case of straight lines and curves.

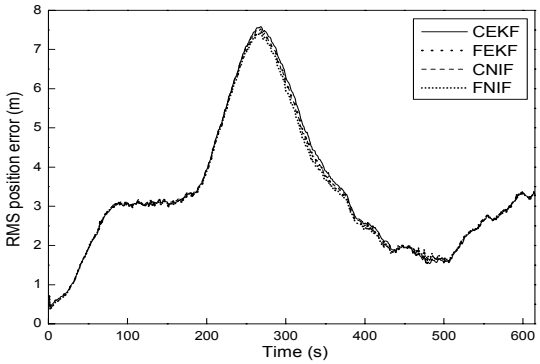

Fig. 4. Comparison of position errors in the case of straight lines and curves.

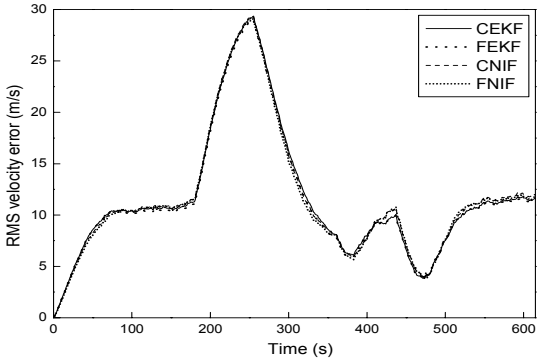

Fig. 5. Comparison of velocity errors in the case of straight lines and curves.

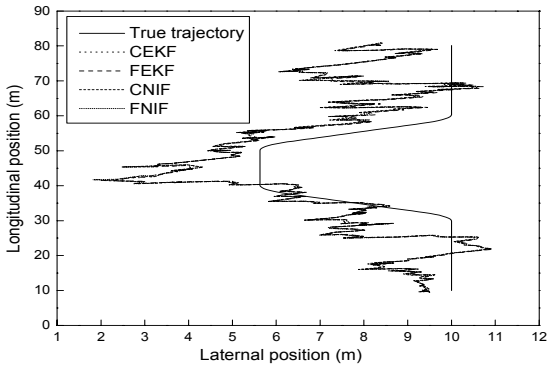

Fig. 6. Comparison of position estimates in the case of cut-in/out.

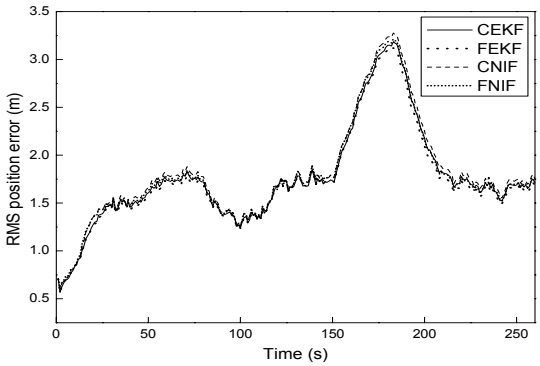

Fig. 7. Comparison of position errors in the case of cut-in/out.

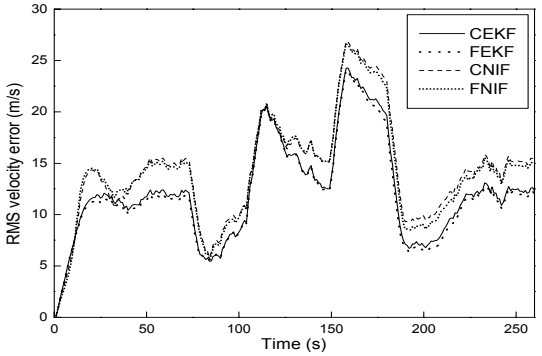

Fig. 8. Comparison of velocity errors in the case of cut-in/out.

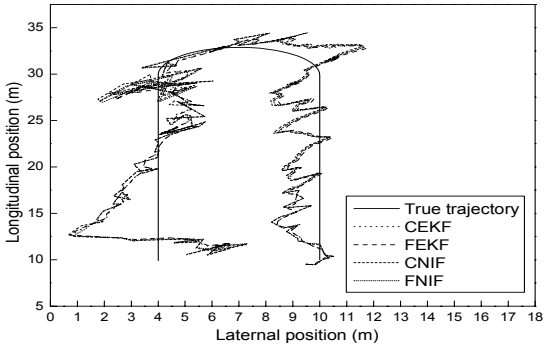

Fig. 9. Comparison of position estimates in the case of u-turn.

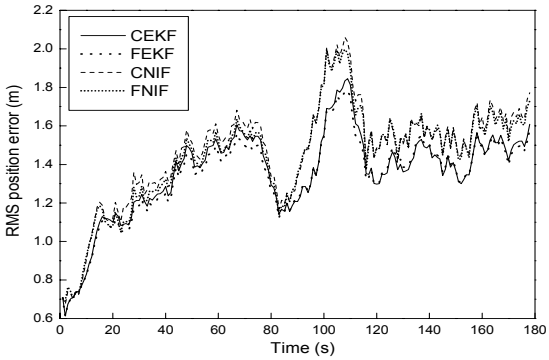

Fig. 10. Comparison of position errors in the case of u-turn.

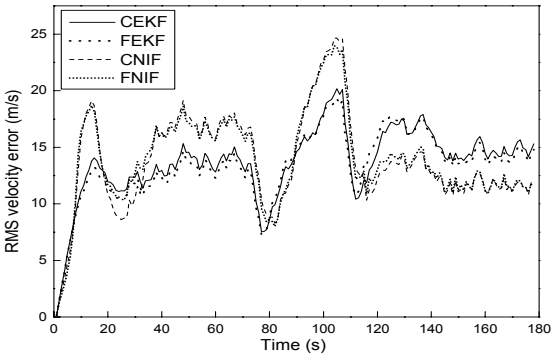

Fig. 11. Comparison of velocity errors in the case of u-turn.

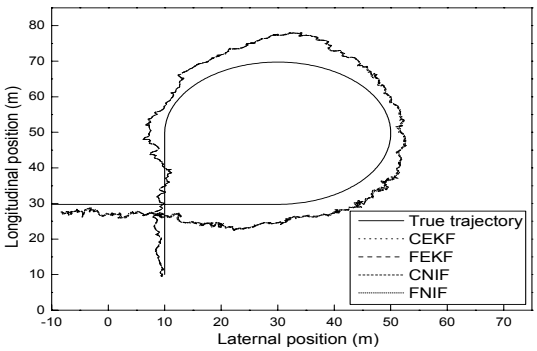

Fig. 12. Comparison of position estimates in the case of interchange.

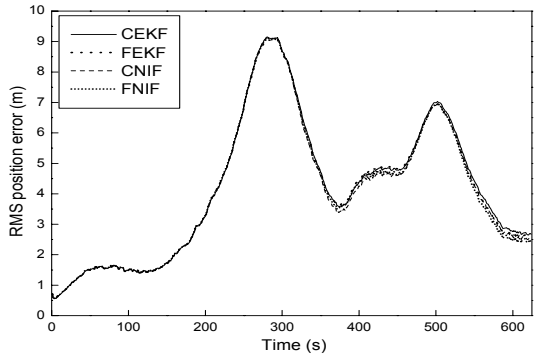

Fig. 13. Comparison of position errors in the case of interchange.

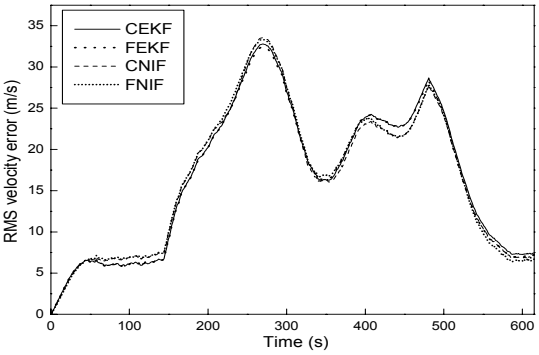

Fig. 14. Comparison of velocity errors in the case of interchange.

5. CONCLUSIONS

In this paper, a tracking algorithm to track a maneuvering vehicle on a road in an adaptive cruise control environment was designed. The tracking algorithm detects and tracks other maneuvering vehicle on a road by two kinematic models derived in this paper. For the constant-speed turn model, a federated nonlinear information filter was used in place of the extended Kalman filter in multi-sensor systems. Besides, it was mathematically shown that, in view of the information sharing factor, the federated information filter is equal to the centralized information filter. Comparison and analysis of the

IMM algorithms using the CEKF, the FEKF, the CNIF, and the FNIF were performed.

REFERENCES

[1] Y. Bar-Shalom, X. Li, and T. Kirubarajan, *Estimation with Applications to Tracking and Navigation*, John Wiley & Sons, INC, New York, 2001.

[2] N. A. Carson, "Federated square root filter for decentralized parallel processes," *IEEE Transactions on Aerospace and Electronic Systems*, vol. 26, no. 3, pp. 517-525, 1990.

[3] N. A. Carlson and M. P. Berarducci, "Federated Kalman filter simulation results," *Journal of the Institute of Navigation*, vol. 41, no. 3, pp. 297-321, 1994.

[4] D. S. Caveney, *Multiple Target Tracking in the Adaptive Cruise Control Environment Using Multiple Models and Probabilistic Data Association*, M. S. Thesis, University of California, Berkeley, U. S. A., 1999.

[5] K. C. Chang, T. Zhi, and R. K. Saha, "Performance evaluation of track fusion with information matrix filter," *IEEE Trans. on Aerospace and Electronic Systems*, vol. 38, no. 2, pp. 455-466, 2002.

[6] C. Y. Chong, S. Mori, and K. C. Chang, "Distributed multitarget multisensor tracking," in Bar-Shalom, Y. (Ed.), *Multitarget-Multisensor Tracking: Advanced Applications*, Artech House, Norwood, MA, 1990.

[7] F. Dufour and M. Mariton, "Passive sensor data fusion and maneuvering target tracking," in: Bar-Shalom, Y. (Ed.), *Multitarget-Multisensor Tracking: Applications and Advances*, Artech House, Norwood, MA, Chapter 3, pp. 65-92, 1992.

[8] J. P. Helferty, "Improved tracking of maneuvering targets: The use of turn-rate distributions for acceleration modeling," *IEEE Trans. on Aerospace and Electronic Systems*, vol. 32, no. 4, pp. 1355-1361, 1996.

[9] V. P. Jilkov, D. S. Angelova, and TZ. A. Semerdjiev, "Design and comparison of mode-set adaptive IMM algorithms for maneuvering target tracking," *IEEE Trans. on Aerospace and Electronic Systems*, vol. 35, no. 1, pp. 343-350, 1999.

[10] Y. S. Kim and K. S. Hong, "An IMM algorithm for tracking maneuvering vehicles in an adaptive cruise control environment," *International Journal of Control, Automation, and Systems*, vol. 2, no. 3, pp. 310-318, September 2004.

[11] T. G. Lee, "Centralized Kalman filter with adaptive measurement fusion: its application to a GPS/SDINS integration system with an additional sensor," *International Journal of Control, Automation, and Systems*, vol. 1, no. 4, pp. 444-452, December 2003.

[12] B. J. Lee, Y. H. Joo, and J. B. Park, "An Intelligent tracking method for a maneuvering target," *International Journal of Control, Automation, and Systems*, vol. 1, no. 1, pp. 93-100, March 2003.

[13] S. J. Lee, J. H. Hong, and K. S. Yi, "A modeling and control of intelligent cruise control systems," *Trans. of the KSME, A*, vol. 25, no. 2, pp. 283-288, 2001.

[14] X. Li and Y. Bar-Shalom, "Design of an interacting multiple model algorithm for air traffic control tracking," *IEEE Trans. on Control Systems Technology*, vol. 1, no. 3, pp. 186-194, 1993.

[15] I. K. Moon and K. S. Yi, "Vehicle tests of a longitudinal control law for application to stop-and-go cruise control," *KSME International Journal*, vol. 16, no. 9, pp. 1166-1174, 2002.

[16] A. G. O. Mutambara, *Decentralized Estimation and Control for Multisensor Systems*, CRC Press, Boca Raton, 1998.

[17] E. Semerdjiev and L. Mihaylova, "Variable- and fixed-structure augmented interacting multiple-model algorithms for maneuvering ship tracking based on new ship models," *International Journal of Applied Mathematics and Computer Science*, vol. 10, no. 3, pp. 591-604, 2000.

[18] Y. Zhu, Z. You, J. Zhao, K. Zhang, and X. Li, "The optimality for the distributed Kalman filtering fusion," *Automatica*, vol. 37, no. 9, pp. 1489-1493, 2001.

Yong-Shik Kim was born in Busan, Korea, on November 24, 1970. He received the B.S. degree in Mechanical Engineering from Donga University, Busan, Korea, in 1994 and the M.S. degree in Mechanical and Intelligent Systems Engineering from Pusan National University, Busan, Korea, in 2000. And he received the Ph.D. degree in the Department of Mechanical and Intelligent Systems Engineering at Pusan National University, Busan, Korea, in 2005. He is currently a postdoctoral researcher in Graduate School of Systems and Information Engineering at University of Tsukuba, Japan. His research interests include estimation theory, target-tracking systems, sensor fusion, fault detection, and localization and obstacle detection of a mobile robot.

Keum-Shik Hong for photograph and biography, see p. 67 of the March 2004 issue of this journal.